

## MISSILE ENDGAME ANALYSIS VIA MULTIOBJECTIVE OPTIMIZATION

N. Patel, A. J. Chipperfield and A. J. Keane

*School of Engineering Sciences, University of Southampton,  
Highfield, Southampton, Hampshire, England SO17 1BJ*

**Abstract:** The traditional approach to improving the lethality of a missile has been to concentrate efforts in the guidance and control systems to improve accuracy and agility. In this paper, we consider how optimizing the endgame, the final few milliseconds before detonation, can yield improvements in overall lethality. As there is likely to be uncertainty in both the target parameters and missile coordinates, a multiobjective problem is developed so that the robustness of a solution can be traded against its efficacy. The ability to quickly determine promising endgames is likely to be of benefit when exploiting modern control schemes, such as MPC, that offer improved accuracy and agility. *Copyright © 2005 IFAC*

**Keywords:** Endgame optimization, guidance and control, aerospace systems, Gaussian functions.

### 1. INTRODUCTION

The present generation of missile systems are likely to be sub-optimal in many engagement scenarios currently considered. Examples of engagements include both anti-air and ground attack domains and these have to allow for an increased use of stealth, more effective countermeasures and the use of redundant subsystems for increased mission survivability. Traditionally, improvements in missile lethality have been sought through improved guidance and control laws, for example, to optimize guidance for a specific control law and engagement conditions (Gurfil, 2001) or by solving receding horizon optimizations to achieve fast and realisable online target tracking (Kim *et al*, 2001). In this paper, the focus is on optimization of the endgame, i.e., the reachable set of outcomes in terms of engagement geometry, rather than the guidance and control laws that result in such a state being achieved.

Flyout is the portion of flight from release to immediately before detonation. During flyout the missile has to engage the target and deliver the warhead to within a close distance of the target. The engagement geometry at the start of the endgame is

critical to the lethality and is the state at the end of flyout. The next section describes how the endgame can be modelled and a programme (AGILE) for achieving that is briefly described. The use of optimization to enhance the lethality of endgames is then considered and further developed with multiobjective formulations to find endgames that have a high probability of kill as well as robustness to variations in the parameters of the problem.

### 2. ENGAGEMENT MODELLING

The trajectories and orientations of the missile and target in the final milliseconds before detonation are collectively known as the endgame geometry. Consider the missile-target engagement shown in Fig. 1. Using GW372 notation (Payne, 1995) the relationship between the Cartesian frames of reference for the missile and the target can be defined where the  $x$ ,  $y$  and  $z$  axes are usually aligned in both frames as follows:

- The  $x$ -axis is to the left (e.g., along the port wing of a fixed-wing aircraft);
- The  $y$ -axis is up (in level flight, the direction of the pilot's torso);

- The z-axis is ahead, along the centre line of the aircraft or missile (i.e., in direction of flight with zero incidence).

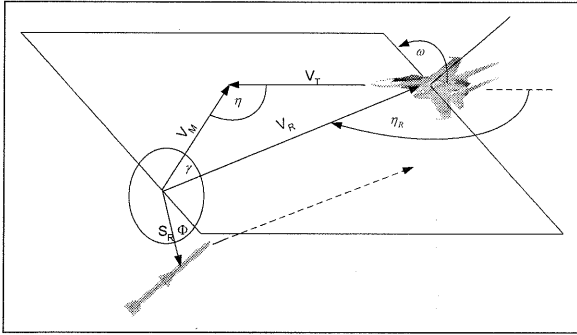


Fig. 1: Engagement geometry in GW372 notation.

The GW372 coordinates only specify relative position, velocity and orientation. Higher derivatives, e.g., acceleration and rotation rates, are not required as lethality is not usually sensitive to them due to the very short time periods involved in damage mechanisms. All angles in GW372 are specified in degrees and from Fig. 1 the following are identified:

- $V_m$  and  $V_t$  are missile and target speeds (m/s).
- $\eta$  is the engagement angle that is subtended between the missile and target velocity vectors ( $\eta = 0 \rightarrow$  tail chase,  $\eta = 180^\circ \rightarrow$  head-on).
- $\omega$  is target roll.
- $\delta$ ,  $\varepsilon$ , and  $\psi$  define missile yaw, pitch and roll.
- $\phi$ ,  $S_r$ , and  $z$  define the missile burst points.  $\phi$  is known as the dartboard angle,  $S_r$  is the dartboard radius and  $z$  specifies the position of the burst point along the trajectory.
- Additional parameters,  $x_0$ ,  $y_0$  and  $z_0$ , define a missile aim point in the target's frame of reference. This point defines the warhead detonation point as the cylindrical polar coordinate system ( $\phi$ ,  $S_r$  and  $z$ ) where the x-axis is aligned with missile velocity.

The important feature of this system is the use of a 'Common Velocity' (CV) plane as a datum for measuring many of the angles in the system. The CV plane is defined as the plane containing the missile and target velocity vectors (or parallel vectors), and passing through the target origin. The CV plane can have any orientation in space. In reality the missile and target both move along their respective velocity vectors; however it is easier to think of the target as stationary with the missile moving along a vector  $V_R$  towards it. It is usually assumed that as the missile approaches the target along  $V_R$  all the other parameters remain constant (no manoeuvre takes place). This assumption is justified because all the fuzing and lethality events take place over a few milliseconds and within a very short distance (a few meters) of the trajectory length. The GW372 system therefore has the advantage that the primary parameters can be changed independently of each other, and each has a clear physical meaning.

A lethality prediction tool, Analytic Gaussian Intersection for Lethality Engagement (AGILE), allows engagements defined using GW372 to be evaluated and a value (probability) of engagement uncertainty, or 'kill probability',  $P_k$  determined (Watson, 2003). AGILE can evaluate an endgame geometry in milliseconds, including: prediction of damage inflicted by warhead fragments on the target or target components; a close-burst model incorporating blast effects; direct impact model; and a simple fuzing model.

The principal method of representing the above model features is by using 3-dimensional Gaussian functions. A Gaussian function  $f$  has the following form:

$$f(x) = a \exp \left[ -\frac{1}{2} (x-b)^T C^{-1} (x-b) \right]$$

where  $x$  is a spatial position vector (with three Cartesian components),  $a$  is the maximum value of  $f$ ,  $b$  is the position vector where  $f$  is maximal and  $C$  is a  $3 \times 3$  positive-definite symmetric matrix representing the shape and orientation of level sets (surface contours) of  $f$ . The level sets of a Gaussian are ellipsoids, so the Gaussian itself can be thought of as a fuzzy ellipsoid; the value of  $f$  decays smoothly from  $a$  to zero as the distance from the centre  $b$  of the ellipsoids increases.

The following objects are represented by sums of Gaussian functions in AGILE:

- Target vulnerability to warhead fragment damage. Regions of high vulnerability are close to the centre of one of more Gaussians, whilst regions of low or zero vulnerability are typically further away from the centres.
- Warhead fragment cluster density. This is not the density or mass of individual fragments, but their average number per unit volume, or 'population density'. Where the target vulnerability and warhead fragment density are both high, the level of damage (probability of target kill or component failure) will be high.
- Close-burst lethality and warhead blast damage. A set of ellipsoids and cylinders is used to define a neighbourhood of the target for which a 'kill' is certain. This neighbourhood is the set of all points inside one of more of these objects; the latter are derived from level sets (contour surfaces) of Gaussian functions.
- Target shape, which is used by both the fuzing and impact models. In the fuzing model Gaussians are used to define the external shape of the target and its reflectivity to the radiation used by the fuzing sensor. In the impact model Gaussians are used to define the shape of both the missile and target, so that the severity of a collision can be calculated.
- Missile shape. Used by the impact model.
- Radiation pattern of the fuzing sensor. This information is used in conjunction with the

shape and reflectivity of the target to predict the moment when the fuze is triggered.

Gaussian components are used in AGILE for the following reasons:

- Their intersections can be computed very efficiently using an analytical formula, hence the acronym Analytic Gaussian Intersection for Lethality Engagement.
- Uncertainty in the endgame geometry can be represented directly by Gaussian components, reducing or avoiding the need for Monte-Carlo methods.

The reason for AGILE's speed is its ability to represent many warhead fragments as a single entity; instead of computing the intersection of each fragment with the target, a single calculation can be applied to hundreds of fragments as an ensemble. Fig. 2 shows an example of an endgame for a simple fixed-wing target. Here, the engagement angle  $\eta = 46^\circ$ , represents a rear, side-on impact at a miss-distance of 15m. From the fragment trajectories, it can be seen that for this endgame geometry, the port wing is vulnerable to fragment damage while the rest of the aircraft remains unshaved. AGILE evaluates kill probabilities from the Gaussian components described above assigning an overall probability of kill,  $P_k$ , and individual probabilities for a kill arising from cockpit, fuselage, engine and wing damage. Clearly, in Fig. 2 the majority of the  $P_k$  arises from fragments damaging the wing and its components.

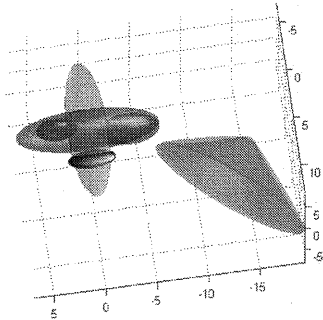


Fig. 2: Fragment vulnerability for simple fixed-wing aircraft.

The parameters listed in Table 1 can be varied over the ranges shown in an AGILE endgame evaluation. Fig. 3 shows the result of exercising AGILE with 1000 input sets where the values for the parameters are chosen randomly over these ranges. It is clearly unlikely that a random endgame will yield a high value of  $P_k$ . By optimizing the endgame geometry to achieve high and/or robust  $P_k$ , the missile flyout endpoint is determined and a suitable guidance law can be developed using conventional approaches such as Shinar & Vladimir (2003) or intelligent ones such as Leng (1996).

In the next section, a series of optimizations are employed to determine good engagement geometries. The engagement space is first sampled and direct

optimization of the probability of kill considered through a restricted parameter set. However, a requirement of a good endgame is that the probability of kill should be robust to uncertainty in the parameters. Thus, multiobjective optimization is used to identify such solutions and their properties assessed.

Table 1: Agile engagement parameters

Parameter	Min	Max	Nominal
$V_M$	0	2000	-
$V_T$	0	2000	-
$\eta$	0	180	-
$S_R$	0	100	15
$\omega$	0	360	0
$\delta$	0	180	0
$\varepsilon$	0	180	0
$\psi$	0	360	0
$x_0$	-5	5	0
$y_0$	-5	5	0
$z_0$	-5	5	0
$Z_{delay}$	-10	10	0

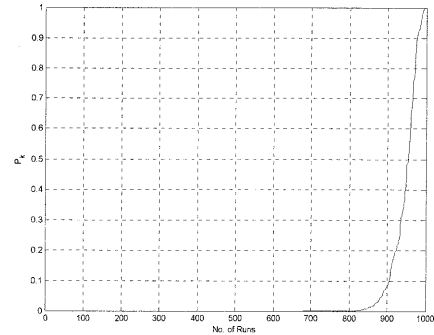


Fig. 3: Random search  $P_k$  distribution.

### 3. ENDGAME OPTIMIZATION

The endgame is the final few milliseconds of flight before detonation of the warhead. In order to maximize the probability of a kill, the missile guidance system must ensure that the missile parameters approach those of a suitable endgame. Alternatively, achieving the maximum  $P_k$  given a limited deviation from a nominal endgame might be a suitable goal for a model-based predictive controller used in the guidance loop. The following four problems explore the use of AGILE as a tool for determining and maximizing endgame lethality.

#### Problem 1: max $P_k$

The three most significant parameters affecting the endgame are missile speed,  $V_M$ , target speed,  $V_T$ , and the missile-target engagement angle,  $\eta$ . The single objective considered is min ( $-P_k$ ) and Table 2 shows ten examples of achievable  $P_k$  given the starting point  $\{V_{M_i}, V_{T_i}, \eta_i\}$ . These optimizations were performed

using the SQP algorithm in the MATLAB Optimization Toolbox with the remaining parameters set to the nominal values of Table 1. The initial sets are not always sensible, but demonstrate how the engagement geometry should be modified to improve potential lethality. For example the initial set  $\{1400, 1600, 0\}$  represents a tail-chasing missile travelling slower than its target. However, given that it is detonated 15 m from the tail of the target, the low probability of kill, 0.366, arises mostly from fragment damage to the engine. By slowing the target to 1465 m s<sup>-1</sup>, increasing the missile speed to 1538 m s<sup>-1</sup> and engaging at a slight incidence of 1.2°,  $P_k$  increases to 0.967.

Table 2: Three parameter engagement geometry optimizations

$V_{Mi}$	$V_{Ti}$	$\eta_i$	$P_{ki}$	$V_M$	$V_T$	$\eta$	$P_k$
750	500	90	0.619	767	300	66.8	0.912
1000	500	90	0.418	800	322	65.7	0.906
1000	600	90	0.441	899	400	63.3	0.885
1300	900	60	0.494	1243	700	55	0.797
1700	1100	30	0.45	1681	1119	24.4	0.509
1400	1600	0	0.366	1538	1465	1.2	0.967
1800	1200	15	0.281	1798	1201	4.4	0.922
1000	500	0	0.607	1000	500	5.2	0.937
1000	500	75	0.546	800	322	65.7	0.906
1800	1300	50	0.288	1651	1100	46.9	0.681

The first three endgames in Table 2 represent side-on engagement. In all three cases, increasing the difference in speed between the missile and target and engaging more towards tail-chase significantly improves  $P_k$ . Fig. 4 shows the variation in  $P_k$  with  $V_M$  and  $\eta$  about the optimized set  $\{V_M, V_T, \eta\}$  from the first row of Table 2 for fixed  $V_T = 300$  m s<sup>-1</sup>. Similarly, Fig. 5 shows how  $P_k$  varies with  $V_T$  and  $V_M$  for a fixed  $\eta = 66.8^\circ$ . These two figures confirm what would be expected during an engagement, namely that maximum lethality will occur at an angle and missile-target speed ratio such that fragment damage is focused on the more vulnerable areas.

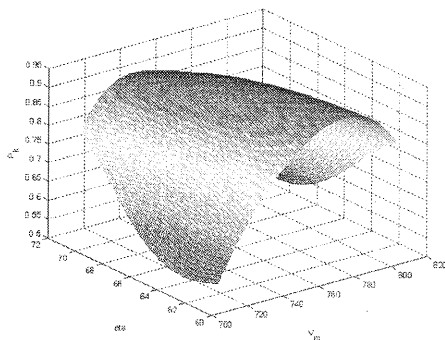


Fig. 4: Variation in  $P_k$  for fixed  $V_T = 300$  m s<sup>-1</sup>.

Figs. 6 and 7 show lethality plots for the engagement of the eighth row of Table 2. The plots are in quite a different area of the permissible engagement space

than those of Figs 4 and 5 although the plots show similar characteristics.

Note though that while the engagement of Fig. 4 is relatively insensitive to angle, that of Fig. 6 is very sensitive to variation in engagement angle. Thus a small error in engagement angle in the first case will result in only a small reduction in  $P_k$ , in the second case the same small change in  $\eta$  could result in  $P_k$  of less than 0.4.

In realistic engagement problems, the target is not completely known and the feedback measurements will be imperfect. The engagement will be also subject to exogenous disturbances. Although these unknowns can be accommodated to some degree in the Gaussians modelling the engagement, it is also important to understand the sensitivity of solutions to parameter uncertainty. In practise this can be achieved by sampling around an 'optimal' solution by, say, taking 100 samples uniformly distributed at random by perturbing the parameters within a percentage of full-scale as depicted in Fig. 8.

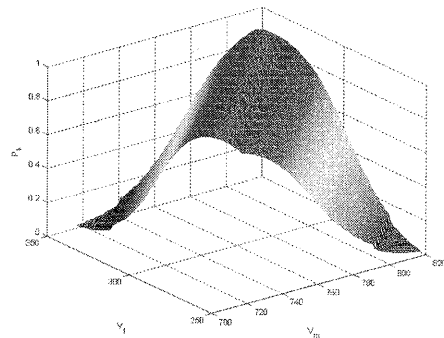


Fig. 5: Variation in  $P_k$  for fixed  $\eta = 66.8^\circ$ .

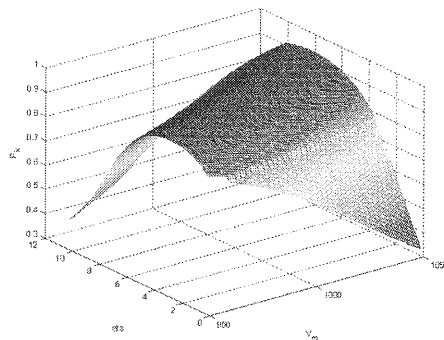


Fig. 6: Variation in  $P_k$  for fixed  $V_T = 500$  m s<sup>-1</sup>.

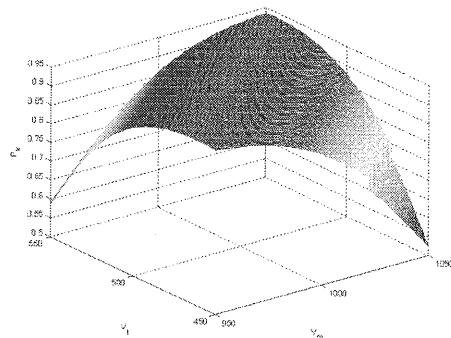


Fig. 7: Variation in  $P_k$  for fixed  $\eta = 5.2^\circ$ .

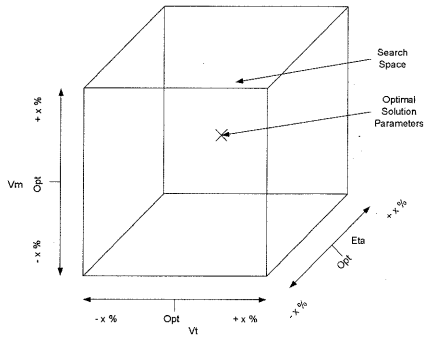


Fig. 8: Perturbation for robustness trade.

**Problem 2:** max  $P_k$  and check for robustness

In practise, a realistic endgame, and therefore flyout, is unlikely to be achievable using only  $\{V_M, V_T, \eta\}$ , not least because the target velocity is unlikely to be under the control of the missile. In this example all parameters in Table 1 are used and the missile's controllable parameters, i.e.  $\delta, \epsilon, x_0, y_0, z_0,$  and  $Z_{delay}$ , are optimized to determine suitable endgames for engaging targets grouped in either head-on, side-on or tail-chase categories, based on engagement angle. The same SQP used in Problem 1 is kept, and 500 scenarios were calculated for each engagement category. For each scenario the optimised parameters are then perturbed 1000 times and the resultant standard deviation of  $P_k$  is recorded.

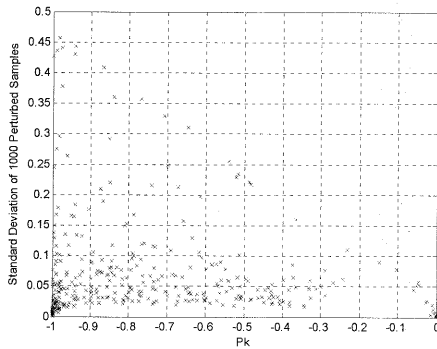


Fig. 9: Scatter plot of head-on engagements and variance (standard deviation) with 10% uncertainty.

As can be seen in Fig. 9, a pair of scenarios with similar  $P_k$ 's can have varying robustness values. As well as maximizing  $P_k$ , it is also desirable to maximize the robustness of the solution to uncertainty in the parameters. Minimizing the standard deviation in the sample is the equivalent of minimizing loss in  $P_k$  due to parameter variations. Attempting to maximize  $P_k$  while simultaneously minimizing the standard deviation should result in endgames that have both a high probability of kill and a high-degree of robustness to parameter uncertainty.

**Problem 3:** max  $P_k$  min  $s(P_k)$  using novel methods

This problem was addressed with a multiobjective genetic algorithm, as described by Fonseca and Fleming (1998), to determine fitness on the basis of non-dominance of the individuals. A MOGA was attractive as the population-based nature of the search

allows many endgames to be evaluated at each generation. The objectives used to assess the performance being (i) overall  $P_k$  as used in problem 1, and (ii) robustness of  $P_k$  calculated as described above. In the example presented here, a  $\pm 10\%$  uncertainty is assumed on the free parameters. In Fig. 10 individual endgames are plotted with their  $P_k$  against the standard deviation in 20 samples around that point in  $\{V_M, V_T, \eta\}$ . Clearly, a fairly large number of high  $P_k$  solutions appear to offer robust endgame performance.

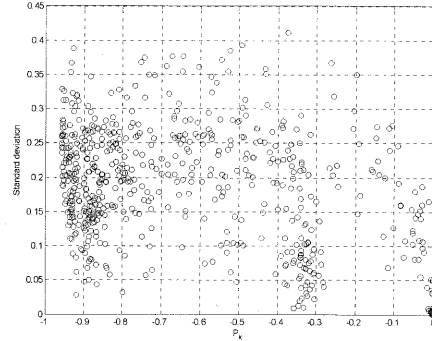


Fig. 10: Scatter plot showing  $P_k$  and variance in  $P_k$  (standard deviation) with 10% uncertainty.

The trade-off between robustness and lethality is shown in Fig. 11 and for the lowest variance sample at  $P_k = 0.9189, s = 0.0298$  the endgame is illustrated in Fig. 12. Improving  $P_k$  to 0.9569 results in an increase in variance to  $s = 0.25$ . A choice of which was the best  $P_k$  would have to be made on a number of factors including: time to endgame; precision of missile; and target vulnerability. The flyout to arrive at an endgame will also have uncertainties arising from the usual modelling considerations, but may also account for target manoeuvring.

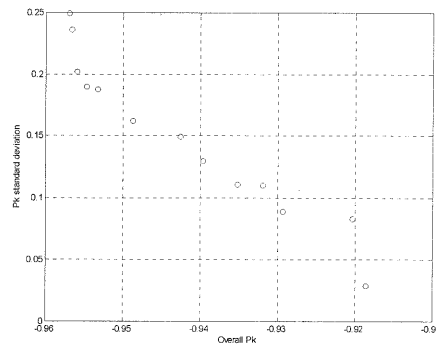


Fig. 11: Trade-off between  $P_k$  and endgame robustness.

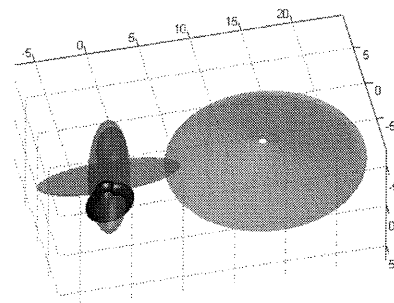


Fig. 12: Robust endgame with  $P_k = 0.9189$ .

The engagement shown in Fig. 12 has  $V_M = 1214$ ,  $V_T = 705$ ,  $\eta = 2.7$  and achieves probabilities of kill of 0.9048 for cockpit damage and 0.1447 for the fuselage. No engine or wing damage is predicted by AGILE. The reason that this is robust to variations in  $\{V_M, V_T, \eta\}$  is the relatively high vulnerability of the cockpit area and the coverage of fragments from the warhead. Such an endgame therefore exploits the characteristics of the missile and the target.

**Problem 4:**  $\max P_k \min s(P_k)$ ,

$$P_k = f(V_M, V_T, \eta, S_R, \omega, \delta, \varepsilon, \psi, x_0, y_0, z_0, Z_d)$$

The same MOGA formulation employed in Problem 3 is retained, and the uncertainty is assumed over all the parameters and the corresponding number of samples at each nominal geometry is increased to 50.

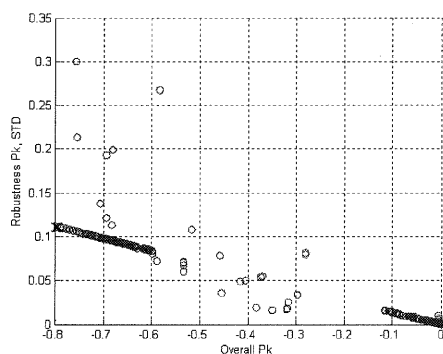


Fig. 13:  $P_k$  vs. robustness trade-off, Problem 4.

The Pareto optimal solutions for side-on scenarios found after 200 generations of 50 individuals are shown in the trade-off of Fig. 13. While similar characteristics can be observed to that of Fig. 11 (Problem 2), in this case the search space is now much larger and hence the greater spread in the solutions. The cross in Fig 13 identifies the endgame shown in Fig 14.

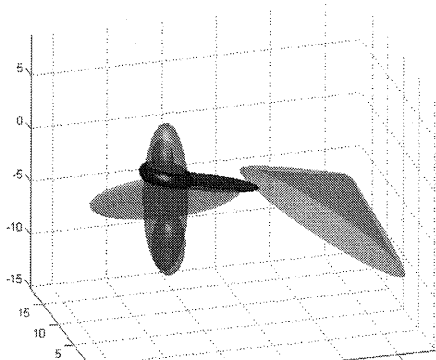


Fig. 14: Engagement with good robustness.

This figure shows an engagement where the missile is approaching fast from towards the aircraft side ( $V_M = 749.91 \text{ m s}^{-1}$ ,  $\eta = 108^\circ$ ) and the missile is oriented  $\{\delta, \varepsilon, \psi\} = \{27^\circ, 209^\circ, -8^\circ\}$  with a burst point (fuze delay) -2 m along the missile trajectory. The overall  $P_k = 0.8$  with 0.7192 cockpit, 0.08 fuselage, and zero engine and wing probabilities of kill. Although a very different endgame to that presented in Fig. 12, the endgame of Fig. 14 is robust in that the fragment

damage to the cockpit is achieved when the missile is detonated within a large region of the 'optimal' point identified in Fig. 13.

#### 4. CONCLUDING REMARKS

This paper has demonstrated how missile endgame conditions with a high probability of kill can be identified using optimization techniques against various performance criteria. There is not one single 'optimal' engagement for a missile-target rather there are families of solutions that trade-off overall lethality with robustness to parameter uncertainty at a number of different condition, for example target speed or engagement angle. Having a better understanding of the location and sensitivity of potential engagement conditions can be readily used in the guidance system to enhance the overall efficacy of the missile which is essential if projected future threats are to be dealt with effectively. The final choice of a suitable endgame will inevitably be a compromise over the criteria and will be determined to some degree by flyout considerations. However, an acceptably accurate simulation, AGILE, can readily and rapidly be used to determine suitable engagement geometries.

#### 5. ACKNOWLEDGEMENTS

The first author wishes to acknowledge the financial and technical support of DSTL throughout this work.

#### REFERENCES

- Fonseca, C. M. and Fleming, P. J. (1998). Multiobjective Optimisation and Multiple Constraint Handling with Evolutionary Algorithms – Part 1: A Unified Formulation. *IEEE Trans. Sys., Man. & Cyber.*, **28**, 26-37.
- Gurfil, P. (2001). Synthesis of zero miss distance guidance via solution of an optimal tuning problem. *Control Engineering Practice* (9) 1117 - 1130.
- Kim, K.B., T.-W. Yoon and W.H. Kwon (2001). Receding horizon guidance laws for constrained missiles with autopilot lags. *Control Engineering Practice* (9) 1107 - 1115.
- Leng, G. (1996). Missile guidance algorithm design using inverse kinematics and fuzzy logic. *Fuzzy Sets & Systems*, (79), 287-295.
- Payne, G.D, (1995). A standard format for the interchange of pass-path geometry data for guided weapon fuzeing and lethality assessments. DRA/WSS/WD5/WP94/29/1.2, UK.
- Shinar, J. and T. Vladimir (2003). What happens when certainty equivalence is not valid? Is there an optimal estimator for terminal guidance? *Annual Reviews in Control* (27), 119-130.
- Watson, G.H. (2003). Agile user guide, QinetiQ, UK.

